

Soil consistency and interparticle characteristics of various biopolymer types stabilization of clay

Zhanbo Cheng and Xueyu Geng*

School of Engineering, University of Warwick, Coventry CV47AL, U.K.

(Received March 26, 2020. Revised April 26, 2021. Accepted September 27, 2021)

Abstract. An environmentally friendly improvement method with using biopolymer stabilization of soil has been currently paid more attention for geotechnical engineering practices. And the existing concerns focused on the performance of biopolymers treated clay due to the occurrence of electrical interaction. Therefore, the effect of biopolymer types and water content on the behaviors of biopolymer-clay mixture should be firstly explored in terms of biopolymer applications. In this study, fall cone tests were conducted to evaluate the consistency variations of eight types of biopolymers treated clay, e.g., carrageenan kappa gum (KG), locust bean gum (LBG), xanthan gum (XG), agar gum (AG), guar gum (GG), sodium alginate (SA), gellan gum (GE) and chitosan (CH) at various biopolymer concentrations (e.g., between 0.1% to 5% biopolymer to soil mass ratio). The results indicated that neutral biopolymers (e.g., LBG and GG) significantly caused the increase of liquid limit and undrained shear strength regardless of biopolymer concentration. And the liquid limit and undrained shear strength of negative charged biopolymers (e.g., KG, SA, GE and XG) treated clay decreased firstly following increased, while AG and CH had limit effect on soil consistency. In addition, the trend of plasticity index was similar to liquid limit altering the USCS classification of biopolymer treated clay as silt or clay. Moreover, empirical equations determining undrained shear strength and shear viscosity of biopolymer-treated clay were also established.

Keywords: biopolymer treated clay; shear viscosity; soil classification; soil consistency; undrained shear strength

1. Introduction

Civil engineering infrastructures were commonly constructed on weak and/or loose soils that required improvement to resist applied loads. Previously, traditional improvement technologies with high mechanical energy and energy-intensive materials (e.g., cement and lime) caused numerous detrimental impacts on the environment problems (e.g., ecosystem contamination, groundwater contamination, ocean pollution and carbon dioxide emission) (Chang *et al.* 2016). For example, the ratio of CO₂ emissions from the cement industry to global CO₂ emissions increased from 2% in 2016 to 8% in 2018 (Andrew 2018). Thus, it is urgent to find out eco-friendly alternatives to replace traditional soil treatment and improvement techniques associated with these environmental concerns.

Microbial induced calcite precipitation (MICP) as the most recognized soil treatment method among biomineralization strategies has been investigated to increase the strength and stiffness of soils (Whiffin *et al.* 2007, DeJong *et al.* 2010). However, a problem in the application of bacteria was that they were slow growing organisms with low rate of exopolysaccharide production and their applications required long-term treatment of soil for its clogging. Secondly, microbial clogging in-situ was that the

penetration of microbial cells in soil depth was limited by the minimum soil pore size from 0.5 to 2 μm (Ivanov and Chu, 2008). Therefore, the method can only be used for soil with suitable hydraulic conductivity. In recent years, biopolymer, as directly utilized biogenic excrement, is characterized as one type of potential eco-friendly material that can be utilised for ground improvement. It shown high performance to improve the soil strength (Viswanath *et al.* 2017, Reddy *et al.* 2018, Chen *et al.* 2019), high ability of erosion reduction against surface water runoff (Ham *et al.* 2018), high water retention and vegetation survivability improvement in drylands (Tran *et al.* 2019), even under a very low concentration (e.g., 0.5%). Especially for fine-grained soil, it can overcome the microbe endocultivation for geotechnical engineering application (Chang *et al.* 2016, Latifi *et al.* 2017, Ni *et al.* 2020, Ni *et al.* 2021).

However, the influence factors of biopolymer-soil matrix formation (e.g., biopolymer type and concentration, soil type, pore-fluid condition and phase transfer with water content variations) should be considered before the application of biopolymers treat soil (Chang *et al.* 2017, Cheng *et al.* 2020). Under high water content, low strength of biopolymer-containing soil can be observed due to the low viscous hydrogel. With the progress of dehydration, soil strength has a significant increase because of the formation of high-tensile-strength biofilms (Lee *et al.* 2017).

The property of mixture soil-water interaction on the particle surface and pore-fluid chemical environmental in pore spaces can be revealed through soil consistency, which also provide essential information to evaluate soil strength (Koumoto and Houlsby 2001). In general, the increased

*Corresponding author, Associate Professor
E-mail: xueyu.geng@warwick.ac.uk

liquid limit corresponded to an increased undrained strength, and vice versa. Nugent *et al* (2009) explained active nanoscale interactions between soil particles, cations, biopolymer and water from five different types of biopolymers treated soil to determine the liquid limit of the treated soil (e.g., XG, GG). Chen *et al* (2013) found that between 0 to 2%, a higher GG concentration led to a higher *LL*, and the same situation for XG with a concentration between 0 to 3%. Furthermore, Chang and Cho (2014) investigated beta-1,3/1,6-glucan treated Korean residual soil experimentally. It was found that a higher glucan content with the concentrations from 0% to 0.8% in the soil raised the *LL* linearly and the *PL* increased slightly from 37.4% to 52%. Subsequently, Chang *et al.* (2019) explored the influence of pore-fluid variation on Atterberg limits of XG treated soils. It can be found that the xanthan gum behavior in the deionized water was governed by clay-mineral type, while the pore-fluid chemistry governed the xanthan gum behavior in the brine and the kerosene.

Have an insight knowledge of soil consistency is important in understanding particle aggregation and water absorption characteristics for geotechnical applications. Nowadays, soil type and pore-fluid conditions have been comprehensively illustrated on the consistency of biopolymer treated soil (Chang *et al.* 2019). Moreover, in terms of clayey soil, biopolymer-to-clay content was more critical than biopolymer-to-total soil content due to electrostatic and chemical bonding characteristics between biopolymers and clay particles. Therefore, the soil consistency of biopolymer treated clay with various biopolymer types and a wide range of biopolymer concentrations should be further explored for geotechnical engineering application.

In this study, eight typically biopolymers (carrageenan kappa gum, KG; locust bean gum, LBG; xanthan gum, XG; agar gum, AG; guar gum, GG; sodium alginate, SA; gellan gum, GE; chitosan, CH) extracted from plants, metastatic products of microorganism, or cell walls of algae easily, as the potential materials in the application of civil engineering infrastructures, were utilized to treat clay with a wide range from 0.1% to 5% concentrations. The aims were to investigate soil behaviors with various biopolymer hydrogels becoming the main pore-filling medium. Specifically, the effect of biopolymer on Atterberg limits, undrained shear strength and shear viscosity were evaluated through experimental tests under various biopolymer types and a wide range of biopolymer concentrations.

2. Materials and method

2.1 Materials

2.1.1 Soil

The Kaolinite used in this experimental study was quarried from the Southwest England. Its plastic limit (*PL*) and liquid limit (*LL*) values were 30.7% and 69.9%, respectively. The specific gravity of the clay grains was found to be 2.6. The clay has been classified as CH based on the Unified Soil Classification System (USCS). And it also belonged to poor gradation. The clay grains were

Table 1 Basic physical parameters of China clay

Soil type	Kaolinite
$D_{60}/\mu\text{m}$	0.976
$D_{50}/\mu\text{m}$	0.74
$D_{30}/\mu\text{m}$	0.4
$D_{10}/\mu\text{m}$	0.247
Specific surface area (m^2/g)	14
C_u	3.95
C_c	0.66
<i>PL</i> /%	30.7
<i>LL</i> /%	69.9
<i>PI</i> /%	39.2
USCS	CH
Specific gravity	2.6

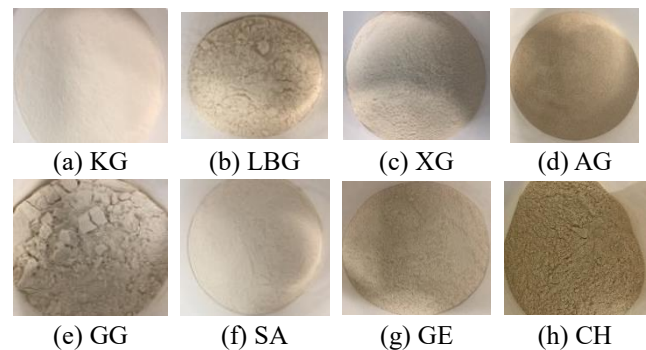


Fig. 1 Biopolymer productions

mainly composed of 47% of SiO_2 and 38% of Al_2O_3 , respectively. Kaolinite can form strong hydrogen bonds with water molecules. Table 1 summarized the specific physical parameters of the Kaolinite.

2.1.2 Biopolymers

In order to provide standardization and practical application, eight biopolymers, e.g. carrageenan kappa gum (KG, CAS No: 90000-07-1), locust bean gum (LBG, CAS No: 9000-40-2), xanthan gum (XG, CAS No: 11138-66-2), agar gum (AG, CAS No: 9002-18-0), guar gum (GG, CAS No: 9000-30-0), sodium alginate (SA, CAS No: 9005-38-3) gellan gum (GE, CAS No: 71010-52-1) and chitosan (CH, CAS No: 9012-76-4) were used in the present study as shown in Fig. 1.

KG was extract from a red algae called kappaphycus alvarezii. It belonged to the carrageenan algae family and was identified to produce gelling, thickening, stabilizing and viscous properties. It was ideal for room temperature gels with soluble in both hot and cold water (van de Velde 2008).

LBG was a galactomannan vegetable gum extracted from the seeds of the carob tree (Barak and Mudgil 2014). LBG was soluble cold but dissolves easier using hot liquids. It can be used to increase the viscosity, thickness and texture of liquids or to produce heat stable gels depending on the dosage.

XG was an anionic and high molecular weight

polysaccharide that was fermented from *Xanthomonas campestris* bacterium (García-Ochoa *et al.* 2000). It was widespread used as a thickener due to its viscous hydrogel formation with the presence of water (García-Ochoa *et al.* 2000).

AG obtained from the cell walls of some species of red algae of the *Gelidiella Gelidium* and *Gracilaria* or red seaweeds (Rhein-Knudsen *et al.* 2015). It was a hydrocolloid, forming a hard, brittle, transparent and neutral gel to provide rigid textures as a stabilizer.

GG was a galactomannan polysaccharide extracted from guar beans that has thickening and stabilizing properties useful in the food and industrial applications. GG was a powerful short texture thickener and can be used even in cold water or liquids (Smitha and Sachan 2016, Cao *et al.* 2018).

SA was the sodium salt form of alginic acid and gum mainly extracted from marine brown algae (Karmakar *et al.* 2009). It can be soluble in cold and hot water with strong agitation. The biggest advantage of alginates was its liquid-gel behavior in aqueous solutions.

GE was a water-soluble anionic polysaccharide produced by the bacterium *Sphingomonas elodea*. It can be used as a thickener, binder, and stabilizer in different food applications (Huang *et al.* 2016). The low acyl gellan gum producing form firm, non-elastic and brittle gel was used in this study.

CH was natural biodegradable and biocompatible polysaccharide, made by treating the chitin shells of shrimp and other crustaceans with an alkaline substance, such as sodium hydroxide (Santos *et al.* 2020). It had excellent moisture absorption, moisture retention, opsonization and bacteria inhibition.

2.1.3 Pore fluid

The chemical composition of the liquid would affect the geotechnical properties of soil (Chang *et al.* 2019). The deionized water was used in the preliminary phase study as pore fluid, so that no additional factors were introduced.

2.2 Sample preparation and testing apparatus

2.2.1 Kaolinite-biopolymer mixture preparation

The clay was completely air dried in an oven at 105°C for 24 hours before a thorough mixing with each dry biopolymer. The biopolymer-to-soil mass ratio (m_b/m_s) for biopolymer-soil mixtures was selected as 0.1-5%. Untreated soil, i.e., pure clay (PC) was also prepared as a reference as shown in Table 2.

2.2.2 Measurement of Atterberg limits

The plastic limit (PL) of biopolymer treated soil was determined following the procedures recommended in ASTM D4318 (ASTM 2017) by rolling out a thread of the soil until its plastic state. On the other hand, fall cone test was conducted to determine the liquid limit (LL) of biopolymer-treated kaolinite by using a cone with 80g weight and 30° tip angle, and a sample cup with 55 mm diameter and 40 mm height (BS 1377 1990). The LL values reflected the water content when the cone penetration depth was 20mm (Wood 1985).

Table 2 Biopolymer treatment conditions

Biopolymers	Concentration (m_b/m_s), %
KG	0, 0.2, 0.5, 1.0, 2.0, 2.5, 3.0, 4.0, 5.0
BG	0, 0.2, 0.5, 1.0, 1.5, 2.0, 2.5, 3.0, 4.0, 5.0
XG	0, 0.1, 0.2, 0.5, 1.0, 2.0, 2.5, 3.0, 4.0, 5.0
SA	0, 0.2, 0.5, 1.0, 2.0, 2.5, 3.0, 4.0, 5.0
GG	0, 0.2, 0.5, 1.0, 2.0, 2.5, 3.0, 4.0, 5.0
AG	0, 0.1, 0.2, 0.5, 1.0, 2.0, 2.5, 3.0, 4.0, 5.0
GE	0, 0.2, 0.5, 1.0, 2.0, 2.5, 3.0, 4.0, 5.0
CH	0, 0.2, 0.5, 1.0, 2.0, 2.5, 3.0, 4.0, 5.0

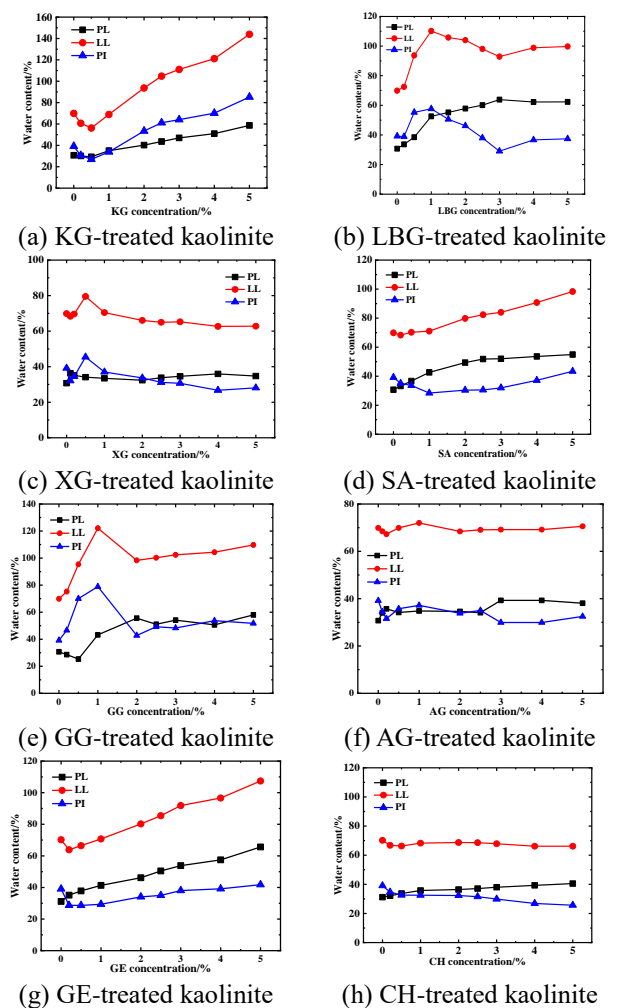


Fig. 2 Consistency limits versus biopolymer concentration

3. Results and discussion

3.1 Determination of Atterberg limits

3.1.1 Results

The relationship between the logarithmic water content (w) and the logarithmic cone penetration (d) was found to be linear for any soil types (Feng 2000, 2001) as given by Eq. (1).

$$\lg w = \lg c + m \lg d \quad (1)$$

where c is the water content at a penetration depth of 1 mm and m is the slope of the linear relationship. The variation of liquid limit, plastic limit and plasticity index ($PI = LL - PL$) with biopolymer contents for soils treated with eight biopolymers were shown in Fig. 2.

As shown in Fig. 2 (a), the plastic limit (PL) of KG treated clay slightly increased from 30.7% to 58.7% with the increase of KG concentration to 5% because the threads of the monomeric molecules made the soil stiffer (Ayeldeen *et al.* 2016). Moreover, the liquid limit (LL) and plasticity index (PI) of KG treated clay can be divided into two stages with the increase of KG concentration. Firstly, the LL and PI of KG treated clay slightly decreased from 69.9% and 39.2% to 56.2% and 26.9%, respectively, at a valley point ($m_b/m_s = 0.5\%$). And then an approximately linear increasing can be observed until 5% KG with the LL and PI increasing to 143.9% and 85.2%, respectively. The LL of 5% KG treated clay was more 2 times than that of untreated clay. Moreover, the increment rate of LL was larger than that of PL after $m_b/m_s > 0.5\%$. Variation of soil consistency with m_b/m_s can be explained with the increase of hydrogel viscosity and the occurrence of particle aggregation induced by KG. As shown in Fig. 3 (a), KG was anionic polysaccharides with consisting of Ester sulphate, Glycosidic linkage, 3,6-anhydro-D-galactose and D-galactose-4-sulphate. It caused kaolinite aggregation via ionic or hydrogen bonding, which accompanied the decrease of surface area reducing the amount of free pore water. Therefore, at lower concentration, the soil consistency reduced due to the particle aggregation and the limited increment of biopolymer solution viscosity in intergranular pores. With the increase of biopolymer concentration ($>0.5\%$), the increase of soil consistency seemed to be attributed to the positive effective of KG hydrogel formation always greater than the simultaneous kaolinite aggregation induced by KG.

In terms of LBG treated clay, the PL slightly increased to 63.8% at 3% LBG concentration and then almost kept constant until 5% LBG concentration as shown in Fig. 2 (b). Moreover, the LL and PI of LBG treated clay increased from 69.9% and 39.1% to 111% and 57.6%, respectively, at 1% LBG concentration. And then both of them reduced to 92.9% and 29% at 3% LBG concentration, respectively, following by almost kept constant until 5% LBG concentration. It can be explained that LBG was a neutral polysaccharide consisting of a polymeric mannose chain branched with galactose units. The main chain consisted of (1-4) linked beta-D mannose residues and the side chain of (1-6) linked alpha-D galactose as shown in Fig. 3 (b). It had numerous hydroxyl groups to form hydrogen bonds between LBG and soil particles inducing particle aggregation to reduce LL. On the other hand, with the increase of LBG concentration, it transformed pore fluids into viscous hydrogel which caused an increase in the viscosity of pore fluids. Therefore, the significant increase of viscosity and the slight particle aggregation at lower concentration caused the great increase of LL. With the increase of LBG concentration, plenty of molecular chains led to hydrogen bonds along with significant particle aggregation reducing the amount of free pore water.

Therefore, LL can be observed some degree of decrease until 3% concentration. And then the behavior of LL for $m_b/m_s > 3\%$ seemed to be attributed the equilibrium between LBG hydrogel formation and the simultaneous kaolinite aggregation induced by LBG. However, it should be noted that LL of LBG treated clay was always larger than that of untreated clay.

The soil consistency of XG treated kaolinite can be illustrated in Fig. 2 (c). LL and PI initially had a slight decrease to 68.4% and 32.1%, respectively, at very low biopolymer content (e.g., 0.1%) following by increased to a peak point with 79.5% and 45.4%, respectively, at 0.5% concentration, and then decreased to an inflection point with 66% and 33.7%, respectively, at 2.0% concentration. The results were in accordance with the previous finding from Chang *et al.* (2019) and Nugent *et al.* (2009). Conversely, the maximum PL with 36.3% can be observed at 0.1% concentration, following by decreased to 32.4% at 2.0% concentration. After that, the soil consistency tended to keep constant with the increase of XG concentration reaching to 5%. As shown in Fig. 3 (c), XG was a long-chain polysaccharide having d-glucose, d-mannose, and d-glucuronic acid with hydroxy and carboxy groups, highly negative charge. At very low XG content (e.g., 0.1%), the change of fluid viscosity can be almost neglected, while the lubrication effect and kaolinite aggregation induced by XG led to a slight decrease of LL. With the increase of XG content, it formed hydrogels with high fluid viscosity in soil pore space, which resulted in the increase of LL with the increment of 14% at 0.5% concentration. However, more XG strands caused the significant particle aggregation via ionic or hydrogen bonding (Laird 1997, Sastry *et al.* 1995), which accompanied a decrease in LL. Moreover, the soil consistency almost kept constant after concentration larger than 2.0% due to the equilibrium between XG hydrogel formation and the simultaneous kaolinite aggregation induced by XG (Nugent *et al.* 2009).

As shown in Fig. 2 (d), PL continuously increased to 51.8% at 2.5% concentration and then remained constant until 5% concentration. The growth rate of PL decreased gradually since SA had strong hydrophilicity. Moreover, it was apparently that only a small valley of LL with 68% was found around 0.2% SA concentration, while the lowest point of PI with 28.4% can be observed at 1% SA concentration. Consequently, LL and PI almost linear increased with the increase of SA concentration to 5% with the values of 98.3% and 48.4%, respectively. SA was a linear polysaccharide derivative of alginic acid comprised of 1,4- β -d-mannuronic (M) and α -l-guluronic (G) acids having hydroxy and carboxyl groups with negative charge as shown in Fig. 3 (d). At the low SA concentration, only slight pore viscosity can be achieved, while the chemical groups and strong ionic characteristics of SA can be interacted with clay with obviously aggregation to reduce surface area and soil pore volume. Therefore, it was observed the slight decrease of LL at 0.2% SA concentration. Moreover, the hydrogel viscosity of SA exponentially increased with the increase of SA concentration contributing to the increase of LL after 0.2% concentration.

In terms of GG treated kaolinite (Fig. 2 (e)), LL and PI initially increased to a peak point with 122.1% and 78.9% at 1% concentration, respectively, and then decreased to an inflection point with 100.3% and 49.2% at 2.0% concentration, respectively, following by a slight increase to 109.7% and 51.8% at 5% concentration respectively. Conversely, PL decreased to 25.3% firstly at 0.5% concentration, following by increased to 55.5% at 2% concentration before approximately keeping constant until 5% concentration. GG was a neutrally charged polysaccharide and its backbone was a linear chain of β 1,4-linked mannose residues to which galactose residues were 1,6-linked at every second mannose with numerous hydroxy groups as shown in Fig. 3 (e). Therefore, it could produce strong hydrogel viscosity by adding small amount of GG and only slight particle aggregation can be observed contributing to the appearance of peak point of LL more 1.7 times than that of untreated clay at 1% GG concentration. However, with the increase of GG, plenty of hydroxy groups can be interacted with clay to form large particle aggregation reducing the absorbed free water in soil pore. And a slight decrease of LL can be observed until 2% concentration, which agreed with the findings from Nugent *et al.* (2009). On the other hand, the hydrogel viscosity had a significant exponential increase after 2% concentration causing the slight increase of LL again. Overall, LL of GG treated clay was always larger than that of untreated clay regardless of GG concentration, indicating the increase of LL caused by increasing pore fluid viscosity outpacing the decrease of LL caused by clay particles aggregation.

As shown in Fig. 2 (f), LL and PI of AG treated kaolinite had a slight decrease to 67.2% and 31.6%, at 0.2% concentration, respectively, while PL increases to 35.7%. And then LL and PL came back to 72% and 37.2% at 1% concentration, respectively. Conversely, PL decreased to 34.8%. With the continuous increase of AG concentration, LL kept constant around 70%. On the other hand, PL and PI had a slight increase and decrease to 39.3% and 29.9%, at 3% concentration, respectively, following by almost remained constant. AG was a linear polymer made up of the repeating unit of agarobiose, which was a disaccharide made up of D-galactose and 3,6-anhydro-L-galactopyranose with numerous hydroxy groups as shown in Fig. 3 (f). And agar solution was slightly negatively charged. However, AG was insoluble in cold water, and AG can form a characteristic gel after soluble hot water with a melting point between 85 to 95°C. Therefore, AG can only slight soluble in the room-temperature water causing a slight change of pore fluid viscosity and particle aggregation. Overall, there was no significant change of AG treated clay consistency compared to untreated clay.

Fig. 2 (g) illustrated the soil consistency of GE treated clay. LL and PI had a slight decrease to 63.9 and 28.7% at 0.2% concentration, respectively, following by increased to 107.4% and 41.8% at 5% concentration, respectively. Meanwhile, PL shown linear increase to 65.7% at 5% concentration. GE was a negatively charged and was composed of tetrasaccharide repeat unit of glucose, glucuronic acid, and rhamnose with lots of hydroxyl groups as shown in Fig. 3 (g). At low concentration (e.g., <0.5%),

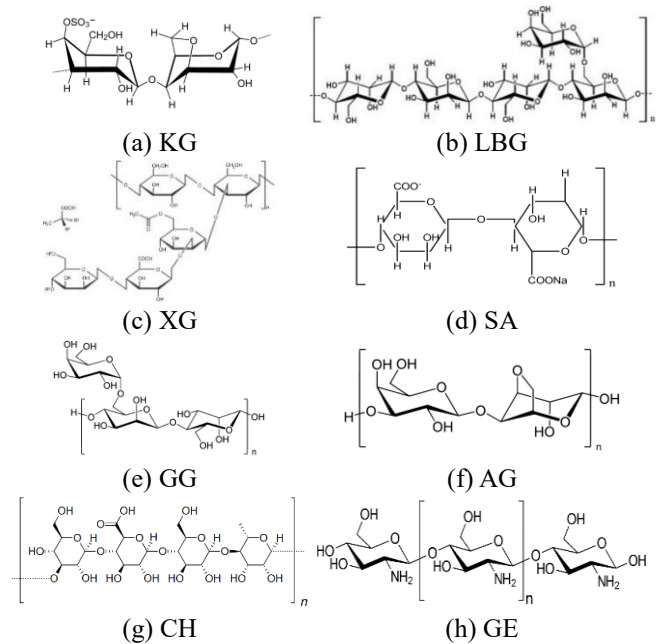


Fig. 3 Chemical structure of various biopolymer type (Dave and Gor 2018, Kang *et al.* 2019)

there was no significant increase for fluid viscosity. Therefore, the particle aggregation caused by ionic or hydrogen bonds led to the decrease of LL. With the increase of GE concentration, the solution viscosity significantly increased overcoming the negative effect of particle aggregation. As a result, LL of 5% GE treated clay was more 1.5 times than that of untreated soil.

As shown in Fig. 2 (h), the LL of CH treated clay decreased to 66.3% at 0.5% concentration and then almost remained constant until 5% concentration. On the other hand, PL continuously increased to 40.5% and PI decreased to 25.6% at 5% CH concentration. CH was a cationic polysaccharide produced by N-deacetylation of its origin with the presence of lots of hydroxyl groups and amino on its surface as shown in Fig. 3 (h). And CH had low solubility and viscosity in water. Therefore, there was only limited particle aggregation via cation bonding or chemical interaction along with the slight decrease of LL at low concentration.

In total, it can be observed that the LL of KG, GE, SA and XG treated clay decreased at the low biopolymer concentration and then increased with the continue increase of biopolymer concentration. And the LL of LBG and GG treated clay increased to the peak point and then decreased following by an equilibrium state with the continue increase of biopolymer concentration. Moreover, there was limited effect on LL of AG and CH treated clay.

3.1.2 Mechanism

Biopolymer mainly interacted with distilled water forming hydrophilic hydrogel on the kaolinite surface and the water absorbed capacity of biopolymer-treated soil can decrease through altering the particle packing of clays (Sridharan *et al.* 1988, Sridharan *et al.* 1999). It was influenced by particle mineralogy, fluid viscosity and the

Table 3 Chemical and physical properties of various biopolymers

Biopolymer	Chemical group	Charge	Soluble in water	MT/°C	Composed
KG	Hydroxyl, hydroxymethyl	negative	Yes	70	repeating galactose units and 3,6 anhydrogalactose
GE	Hydroxyl	negative	Yes	70	tetrasaccharide repeat unit of glucose, glucuronic acid, and rhamnose
SA	Hydroxyl, carboxy	negative	Yes	99	1,4- β -d-mannuronic (M) and α -l-guluronic (G) acids
XG	Hydroxyl, hydroxymethyl, carboxy	negative	Yes	65	d-glucose, d-mannose, and d-glucuronic acid
LBG	Hydroxyl	neutral	Yes	> 90	(1-4) linked beta-D mannose residues and the side chain of (1-6) linked alpha-D galactose β 1,4-linked mannose residues to which galactose residues are 1,6-linked at every second mannose
GG	Hydroxyl	neutral	Yes	80	D-galactose and 3,6-anhydro-L-galactopyranose
AG	Hydroxyl	negative	Yes (insoluble in cold water)	85-95	β -(1 \rightarrow 4)-linked D-glucosamine (deacetylated unit) and N-acetyl-D-glucosamine (acetylated unit)
CH	Hydroxyl	positive	No	102.5	

electro-chemical properties of biopolymer type and concentrations. The chemical and physical properties of various biopolymers can be summarized in Table 3.

Normally, the limit increase of solution viscosity can be observed at low biopolymer concentration causing the limited increase of LL. On the other hand, the strong short-range ionic bond can be immediately formed between charged biopolymer and clay particle. Moreover, biopolymers were polysaccharides with consisting of various chemical groups (e.g., Hydroxyl, hydroxymethyl, carboxy) to form hydrogen bonding with clay. Both of ionic and hydrogen bonding caused particle aggregation to decrease soil surface area. Meanwhile, there was lubrication effect with the occurrence of low biopolymer concentration. All these factors led to reduce the amount of free pore water (Kwon *et al.* 2019). Therefore, it can be illustrated that the LL of KG, GE, SA and XG treated clay decreased at initial stage.

However, with the increase of biopolymer concentration, the viscosity had a significant increase overcoming the negative effective of particle aggregation caused by ionic and hydrogen bonding, which led to the increase of LL. In particle, the maximum LL of KG, GE, SA and XG treated clay was about 2.1, 1.5, 1.6 and 1.14 times than that of untreated soil, respectively. The less of chemical function group sites, short chains and high viscosity of hydrogel of KG contributed to the maximum LL achieved compared to other biopolymers. However, due to the lower solution viscosity, higher electricity, various types and plenty of chemical functional groups of XG compared to other biopolymer types, the maximum LL of XG treated clay can be observed at 0.5% concentration followed by a slight decrease and then had an equilibrium state between XG hydrogel formation and the simultaneous

kaolinite aggregation induced by XG, which was in accordance with the previous findings (Nugent *et al.* 2009, Chang *et al.* 2019).

For the neutral polysaccharide, there was no formation of strong short-range ionic bonding to induce particle aggregation. Therefore, the formation of high viscosity hydrogel due to the occurrence of GG and LBG led to the increase of LL, which was more 1.78 and 1.6 times than that of untreated clay, respectively. Moreover, GG had less chemical functional groups and molecule weight compared to LBG. And GG was more soluble in cold water than LBG due to its extra galactose branch points. Therefore, LL of GG treated clay was larger than that of LBG at the same concentration.

With the increase of GG and LBG concentration, the particle aggregation caused by hydrogen bond can be observed, which offset the positive effect of the viscosity of GG and LBG leading to the decrease of LL after 1% concentration. However, there was limit GG and LBG soluble in room-temperature water with the continuous increase of biopolymer concentration. Therefore, the LL of GG and LBG treated clay tended to remain constant at higher concentration because there was equilibrium state between biopolymer hydrogel formation and the simultaneous kaolinite aggregation caused by chemical functional groups. It was illustrated that the optimum concentration of GG and LBG was 1% to achieve the maximum LL. Interestingly, LL of GG and LBG treated clay was always higher than that of untreated clay regardless of biopolymer concentration because the increase of solution viscosity had dominant effect on the results of LL.

However, AG and CH were limit soluble or even insoluble in room-temperature water, which contributed to

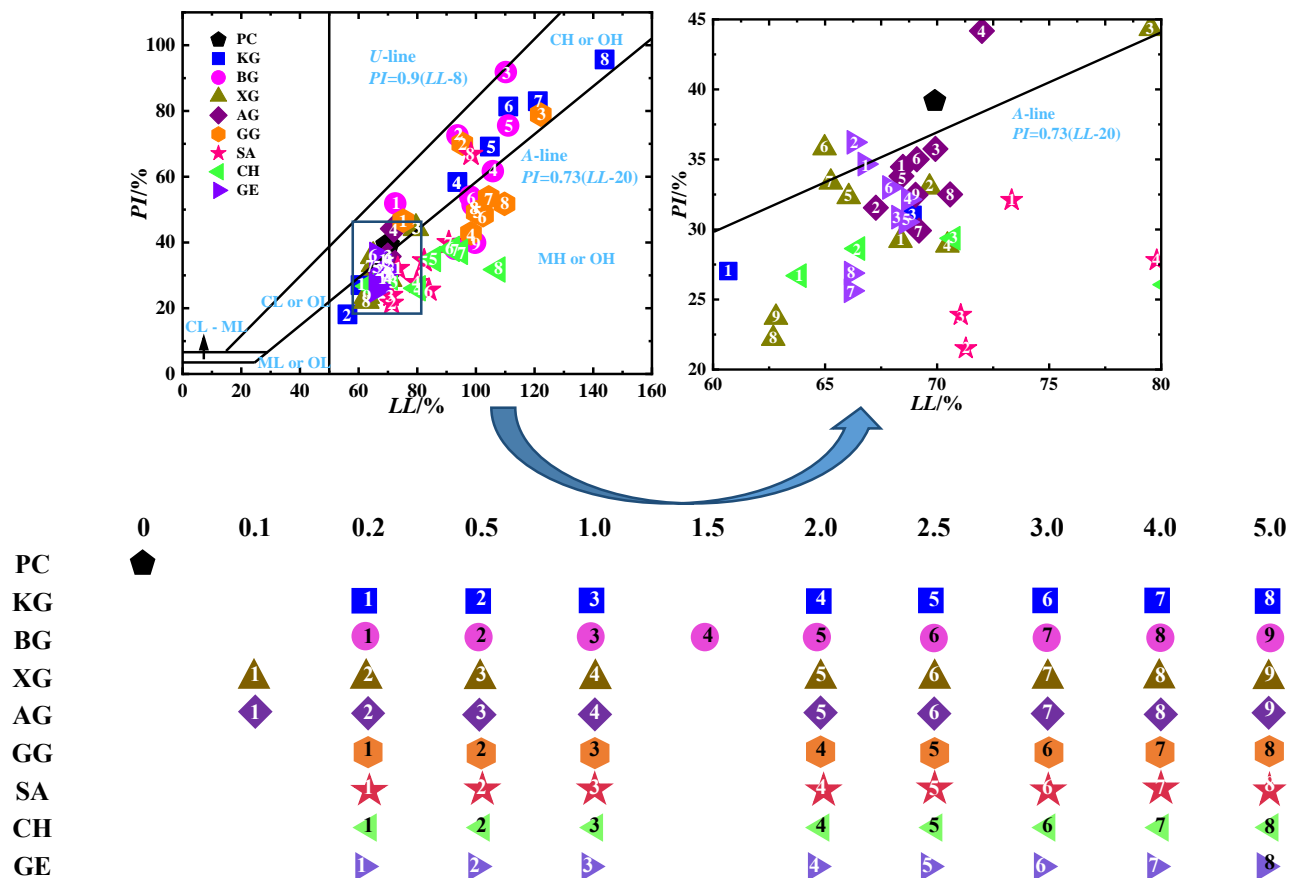


Fig. 4 Chart for the classification of soils used in this study based on USCS

the limit change of LL with the increase of AG and CH concentration. In total, biopolymer had contrary effects on the soil consistency. The difference effectiveness of eight biopolymer types in increasing the LL of kaolinite were attributed to the variety in viscosities of biopolymer hydrogel and aggregation levels of kaolinite particles caused by ionic or hydrogen bonding.

3.1.3 Soil classification

Plasticity index and liquid limit were frequently adopted to classify and estimate the behavior of natural soils in geotechnical engineering. The LL-PI plane was plotted in Fig. 4. It illustrated that most of the samples can be considered as silt falling below *A* line. Others were classified as clay falling between *U* line and *A* line. The soil plasticity tended to increase owing to the biopolymer-induced formation of viscous hydrogel or decrease due to clay particle aggregation. Therefore, both biopolymer types and concentrations contributed to soil classification together.

3.2 Determination of undrained shear strength

The fall cone undrained shear strength of various biopolymer types treated kaolinite with a wide range of biopolymer concentrations was evaluated through the results of fall cone penetration tests. It was conducted to assess the effect of biopolymer types and concentrations on the undrained shear strength at various water contents.

Haosbo (1957) proposed that the undrained shear strength (S_u) can be determined by the cone penetration (d) as shown in Eq. (2).

$$S_u = K \frac{W}{d^2} \quad (2)$$

where W is weight of the cone, 80g; K is no-dimensional fall cone factor, 0.85 (Wood, 1985).

The undrained shear strength of biopolymer-treated kaolinite as shown in Fig. 5 was mainly dependent on the net attractive force and the mode of particle arrangement. With the decrease of water content, the undrained shear strength increased regardless of biopolymer types and concentrations. In terms of LBG and GG treated kaolinite, the undrained shear strength was larger than pure clay regardless of biopolymer concentrations due to these three biopolymers absorbing pore water and forming a viscous hydrogel in pore space to increase the shearing resistance. However, a large number of intermolecular bonds (e.g., electrostatic bonds, van der Waals, ionic-dipole, hydrogen bonds or hydrophobic interactions) between biopolymer and electrically charged kaolinite particles enlarged aggregate size that led to the reduction of undrained shear strength. Therefore, the undrained shear strength of charged biopolymer (e.g., KG, SA, GE and XG) treated kaolinite had a slight decrease at lower concentration. On the other hand, with the increase of biopolymer concentration, the high viscous hydrogel can be formed to increase undrained shear strength. Therefore, the highest undrained shear

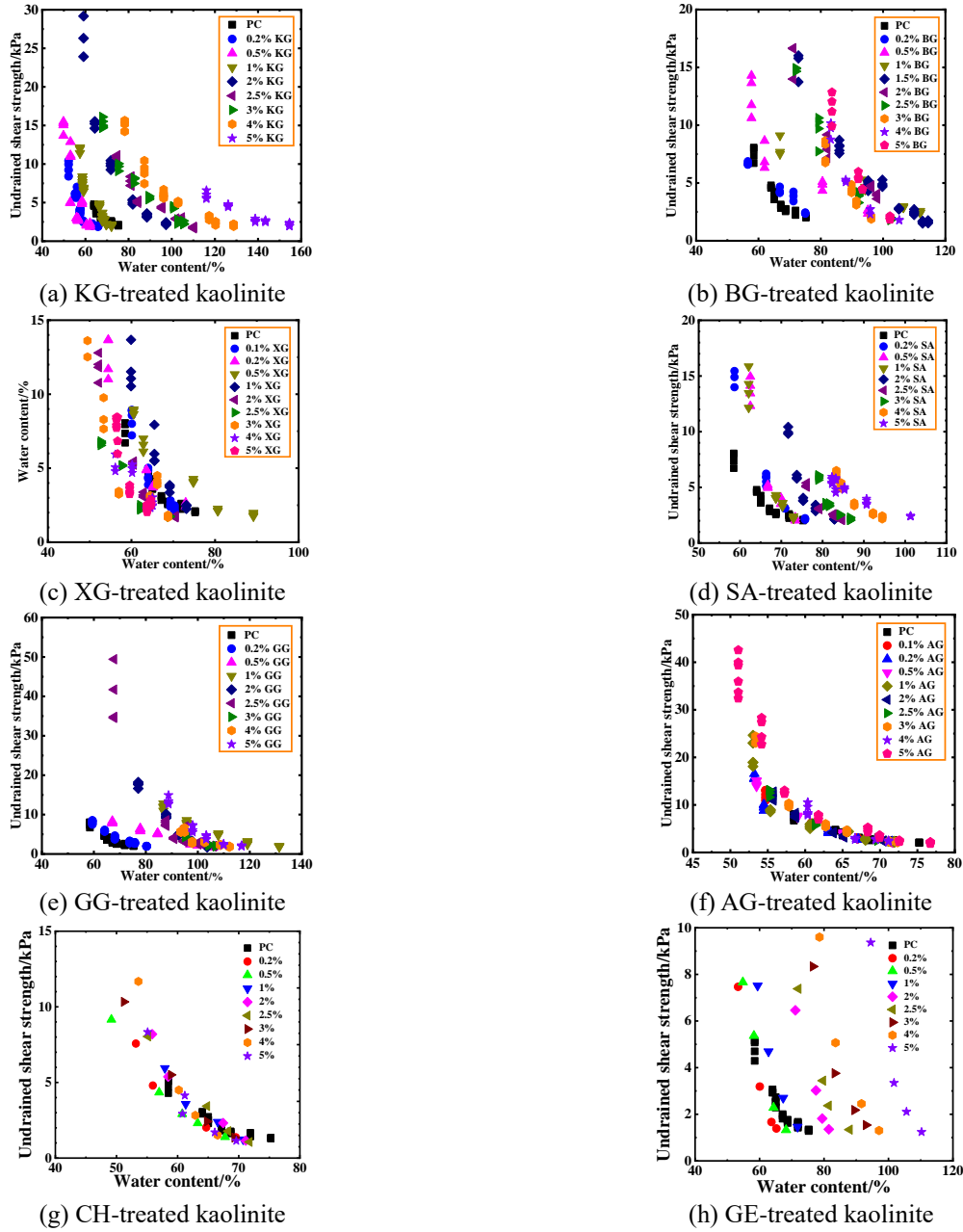


Fig. 5 Undrained shear strength of biopolymer treated clay

strength of XG treated kaolinite can be observed at 0.5% and the undrained shear strength of other biopolymers (e.g., KG, SA and GE) treated clay increased after 0.5% concentration. In addition, there had limit effect on the undrained shear strength of AG and CH treated clay with the increase of biopolymer concentration, which was agreement with the previous results of soil consistency.

Researchers proposed many empirical equations by assuming a logarithmic dependence of undrained strength on liquidity index for biopolymer-treated soil (Chen *et al.* 2013). Based on the best fitting of the test data of S_u versus normalization water content (w/LL) in Semi logarithm scale as shown in Fig. 6, the following equation can be derived to estimate the S_u of biopolymer-treated kaolinite based on the current results of fall cone tests with the coefficient of determination R^2 0.8.

$$S_u = 508.3 \exp(-5.54w/LL) \tag{3}$$

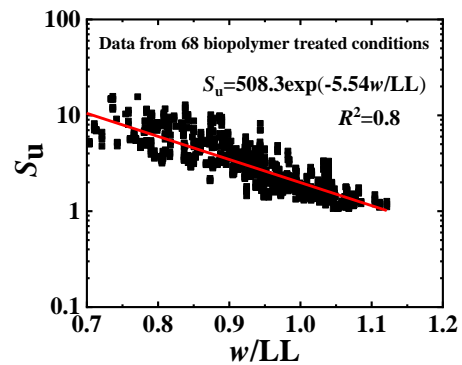


Fig. 6 Undrained shear strength versus normalization water content

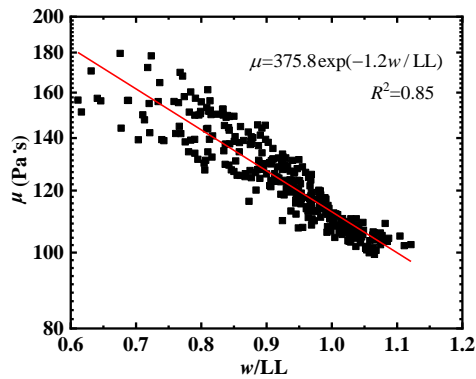


Fig. 7 Shear viscosity versus normalized water content

3.3 Determination of shear viscosity

The viscosity of biopolymer solution was a measure of its resistance to flow at a given rate. For a simple isotropic biopolymer solution, the shear viscosity was defined in terms of the pressure tensor and the shear rate (Mahajan and Budhu, 2009). The shear viscosity (μ) of the soil at dynamic equilibrium can be expressed as follows.

$$\mu = 2.94KW\sqrt{d}\left(\frac{0.67}{h_{eq}} - \frac{1}{d}\right) \quad (4)$$

According to Mahajan and Budhu (2009), the dynamic penetration depth (h_{eq}) can be expressed by cone penetration as follows,

$$h_{eq} = 0.528d + 0.137 \quad (5)$$

The relationship between μ and LI for kaolinite was depicted in Fig. 7. The data can be fitted quite well (regression coefficient = 0.85) by log-log function expressed as follow.

$$\mu = 375.8 \exp(-1.2w/LL) \quad (6)$$

4. Possible implementations and further research

This study assessed the soil consistency and inter-particle characteristics of various biopolymer treated clay. The experimental results indicated that XG, KG, SA and GE can form strong bonds with clay causing particle aggregation and the decrease of surface area. Therefore, all of them tended to have excellent potential for strengthening purposes (e.g., dry condition) on shallow depth stabilization (e.g., soil pavement and slope surface) and controlling hydraulic properties. GG and LBG with high viscosity at low concentration had a significant increase of undrained shear strength, especially with high water content, which were recommend for stabilizing the soft marine soil and controlling surface erosion. CH had potential to coagulate clay as bio flocculant due to insoluble water. Therefore, it can be applied to wastewater treatment, tailings management, land reclamation and soil washing.

For having better performance and a wide range of geotechnical application of biopolymer, some further

studies were recommended to be performed. Obviously, the lower the temperature, the lower the rate at which viscosity increased and the lower the final viscosity. Therefore, it was important to investigate the thermal properties of biopolymer treated soil because biopolymer was only partially soluble in cold water and it normally had high dissolving in hot water for fully hydration. It was expected to increase soil behaviors with the increase of solution temperature.

Furthermore, a large number of free chemical function groups (e.g., hydroxyl and carboxyl groups) were distributed along the biopolymer backbone. These were highly reactive and amenable for chemical modifications. Therefore, the properties like solubility, hydrophobicity and biological characteristics may be altered to have a lot of potential applications of its derivatives. The modifications were accomplished by various chemical processes including oxidation, sulfation, esterification, amidation and graft copolymerization (Yang et al. 2011). For example, the strong KG gel texture was perfect for encasing liquid centers in the presence of calcium, making it perfect for use in dairy proteins (Youssef et al. 2017). And in presence of calcium, sodium alginate can form a gel without the need of heat. On the other hand, strong acids caused hydrolysis and loss of viscosity. Moreover, alkalies in strong concentration also tended to reduce viscosity (e.g., GG) (Venugopal and Abhilash 2010).

In addition, one type of biopolymer can combine with other biopolymers to form cross-link interaction. For example, addition of XG to gelling hydrocolloids, such as KG, AG or LBG, shown to improve gelling property increasing the gel strength and make the typical brittle gels more elastic (van de Velde 2008). However, there need to perform further several tests illustrating the thermal properties of biopolymer, different pore fluid conditions with chemical modifications and the cross-linking of various biopolymers.

5. Conclusion

To study the influences of various biopolymers types and concentrations on the soil consistency and inter-particle characteristics, laboratory experiments were conducted to measure and estimate the soil consistency, undrained shear strength and shear viscosity with eight biopolymers (Carrageenan Kappa Gum, KG; Locust Bean Gum, LBG; Xanthan Gum, XG; Agar Gum, AG; Guar Gum, GG; Sodium Alginate, SA; Chitosan, CH; Gellan Gum, GE) with a wide range from 0% to 5% concentrations. The following conclusions can be drawn.

Biopolymer had contrary effects on the soil consistency. The formation of ionic bond, hydrogen bond and van der Waals force between biopolymer and clay induced particle aggregation decreased the LL of biopolymer treated clay. On the other hand, the LL of biopolymer treated clay can be increased with the formation of high viscosity hydrogel.

The LL and undrained shear strength of neutral biopolymers (LBG and GG) treated clay increased following with decreased and then almost kept constant with the increase of biopolymer concentration, which were

always larger than that of untreated soil regardless of biopolymer concentrations. The LL and undrained shear strength of charged biopolymer (e.g., KG, SA, GE and XG) decreased firstly with the formation of ionic bond induced particle aggregation, and then increased with the appearance of high viscosity hydrogel. Especially, the maximum LL and undrained shear strength of XG treated clay can be observed at 0.5% concentration. However, CH and AG with limit soluble or even insoluble in room-temperature water had limit effect on the clay consistency and inter-particle behaviors.

The PL of biopolymer treated clay increased with the increase of biopolymer concentration. And PI of biopolymer-treated soil was dominated by the LL. Most of biopolymer treated clay were classified as high plasticity silt. For better predicting the undrained shear strength and shear viscosity of biopolymer-treated kaolinite, the newly derived equations based on normalized water content with LL in semi-logarithm scales were proposed, respectively.

Acknowledgments

The authors wish to acknowledge the support from the National Natural Science Foundation of China (51978533, 51608323, 51678319), China Scholarship Council (CSC), Shandong Natural Science Foundation (ZR2016EEM40), European Union's Horizon 2020 research and innovation programme Marie Skłodowska-Curie Actions Research and Innovation Staff Exchange (RISE) (No. 778360).

References

- Andrew, R.M. (2018), "Global CO₂ emissions from cement production", *Earth Syst. Sci. Data*, **10**(1), 195-217. <https://doi.org/10.5194/essd-10-195-2018>
- ASTM 2017 (2017), Standard Test Methods for Liquid Limit, Plastic Limit, and Plasticity Index of Soils. ASTM standard D4318, American Society for Testing and Materials; West Conshohocken, Pennsylvania, U.S.A.
- Ayeldeen, M.K., Negm, A.M. and El Sawwaf, M.A. (2016), "Evaluating the physical characteristics of biopolymer/soil mixtures", *Arab. J. Geosci.*, **9**(5), 371. <https://doi.org/10.1007/s12517-016-2366-1>.
- Barak, S. and Mudgil, D. (2014), "Locust bean gum: processing, properties and food applications-a review", *Int. J. Biol. Macromol.*, **66**, 74-80. <https://doi.org/10.1016/j.ijbiomac.2014.02.017>.
- BS 1377 (1990), Methods of test for soils for civil engineering purposes. Part 2: Classification Tests, British Standards Institution (BSI); London, United Kingdom.
- Cao, J., Jung, J., Song, X. and Bate, B. (2018), "On the soil water characteristic curves of poorly graded granular materials in aqueous polymer solutions", *Acta Geotech.*, **13**(1), 103-116. <https://doi.org/10.1007/s11440-017-0568-7>.
- Chang, I. and Cho, G.C. (2014), "Geotechnical behavior of a beta-1,3/1,6-glucan biopolymer-treated residual soil", *Geomech. Eng.*, **7**(6), 633-647. <http://doi.org/10.12989/gae.2014.7.6.633>.
- Chang, I., Im, J. and Cho, G.C. (2016), "Introduction of microbial biopolymers in soil treatment for future environmentally-friendly and sustainable geotechnical engineering", *Sustainability*, **8**(3), 251. <https://doi.org/10.3390/su8030251>.
- Chang, I., Im, J., Lee, S.W. and Cho, G.C. (2017), "Strength durability of gellan gum biopolymer-treated Korean sand with cyclic wetting and drying", *Constr. Build. Mater.*, **143**, 210-221. <https://doi.org/10.1016/j.conbuildmat.2017.02.061>.
- Chang, I., Kwon, Y.M., Im, J. and Cho, G.C. (2019), "Soil consistency and inter-particle characteristics of xanthan gum biopolymer containing soils with pore-fluid variation", *Can. Geotech. J.*, **56**(8), 1206-1213. <https://doi.org/10.1139/cgj-2018-0254>.
- Chen, C., Wu, L., Perdjion, M., Huang, X. and Peng, Y. (2019), "The drying effect on xanthan gum biopolymer treated sandy soil shear strength", *Constr. Build. Mater.*, **197**, 271-279. <https://doi.org/10.1016/j.conbuildmat.2018.11.120>.
- Chen, R., Zhang, L. and Budhu, M. (2013), "Biopolymer stabilization of mine tailings", *J. Geotech. Geoenviron.*, **139**(10), 1802-1807. [https://doi.org/10.1061/\(ASCE\)GT.1943-5606.0000902](https://doi.org/10.1061/(ASCE)GT.1943-5606.0000902).
- Cheng, Z., Ni, J., Ding, H. and Geng, X. (2020), "Fall cone test on biopolymer-treated clay", *Proceedings of 4th European Conference on Unsaturated Soils*, Lisbon, Portugal, June.
- Dave, P.N. and Gor, A. (2018), "Natural polysaccharide-based hydrogels and nanomaterials: Recent trends and their applications", *Handbook of Nanomaterials for Industrial Applications*, Elsevier, Amsterdam, The Netherlands, 36-66.
- DeJong, J.T., Mortensen, B.M., Martinez, B.C. and Nelson, D.C. (2010), "Bio-mediated soil improvement", *Ecol. Eng.*, **36**, 197-210. <https://doi.org/10.1016/j.ecoleng.2008.12.029>.
- Feng, T.W. (2000), "Fall-cone penetration and water content relationship of clays", *Géotechnique* **50**(2), 181-187. <https://doi.org/10.1680/geot.2000.50.2.181>.
- Feng, T.W. (2001), "A linear log *d*-log *w* model for the determination of consistency limits of soils", *Can. Geotech. J.*, **38**, 1335-1342. <https://doi.org/10.1139/t01-061>.
- García-Ochoa, F., Santos, V.E., Casas, J.A. and Gómez, E. (2000), "Xanthan gum: production, recovery, and properties", *Biotechnol. Adv.*, **18**(7), 549-579. [https://doi.org/10.1016/S0734-9750\(00\)00050-1](https://doi.org/10.1016/S0734-9750(00)00050-1).
- Ham, S.M., Chang, I., Noh, D.H., Kwon, T.H. and Muhunthan, B. (2018), "Improvement of surface erosion resistance of sand by microbial biopolymer formation", *J. Geotech. Geoenviron.*, **144**(7), 06018004. [https://doi.org/10.1061/\(ASCE\)GT.1943-5606.0001900](https://doi.org/10.1061/(ASCE)GT.1943-5606.0001900).
- Hansbo, S. (1957), "A new approach to the determination of the shear strength of clay by the fall cone test", *Royal Swedish Geotechnical Institute Proceedings No.14*, Royal Swedish Geotechnical Institute, Stockholm, Sweden, 7-48.
- Huang, H., Wu, M., Yang, H., Li, X., Ren, M., Li, G. and Ma, T. (2016), "Structural and physical properties of sanxan polysaccharide from *Sphingomonas sanxanigenens*", *Carbohydr. Polym.*, **144**, 410-418. <https://doi.org/10.1016/j.carbpol.2016.02.079>.
- Ivanov, V. and Chu, J. (2008), "Applications of microorganisms to geotechnical engineering for bioclogging and biocementation of soil in situ", *Reviews Environ. Sci. Bio/Technology*, **7**(2), 139-153. <https://doi.org/10.1007/s11157-007-9126-3>.
- Kang, X., Bate, B., Chen, R., Yang, W. and Wang, F. (2019), "Physicochemical and Mechanical Properties of Polymer-Amended Kaolinite and Fly Ash-Kaolinite Mixtures", *J. Mater. Civ. Eng.*, **31**(6), 04019064. [https://doi.org/10.1061/\(ASCE\)MT.1943-5533.0002705](https://doi.org/10.1061/(ASCE)MT.1943-5533.0002705).
- Karmakar, P., Ghosh, T., Sinha, S., Saha, S., Mandal, P., Ghosal, P.K. and Ray, B. (2009), "Polysaccharides from the brown seaweed *Padina tetrastromatica*: Characterization of a sulfated fucan", *Carbohydr. Polym.*, **78**(3), 416-421. <https://doi.org/10.1016/j.carbpol.2009.04.039>.
- Koumoto, T. and Houlsby, G.T. (2001), "Theory and practice of the fall cone test", *Géotechnique*, **51**(8), 701-712.

- <https://doi.org/10.1680/geot.2001.51.8.701>.
- Kwon, Y.M., Chang, I., Lee, M. and Cho, G.C. (2019), "Geotechnical engineering behavior of biopolymer-treated soft marine soil", *Geomech. Eng.*, **17**(5), 453-464. <https://doi.org/10.12989/gae.2019.17.5.453>.
- Laird, D.A. (1997), "Bonding between polyacrylamide and clay mineral surfaces", *Soil Sci.*, **162**(11), 826-832.
- Latifi, N., Horpibulsuk, S., Meehan, C.L., Majid, M.Z.A., Tahir, M.M. and Mohamad, E.T. (2017), "Improvement of problematic soils with biopolymer-An environmentally friendly soil stabilizer", *J. Mater. Civil Eng.*, **29**(2). [https://doi.org/10.1061/\(ASCE\)MT.1943-5533.0001706](https://doi.org/10.1061/(ASCE)MT.1943-5533.0001706).
- Lee, S., Chang, I., Chung, M.K., Kim, Y. and Kee, J. (2017), "Geotechnical shear behavior of xanthan gum biopolymer treated sand from direct shear testing", *Geomech. Eng.*, **12**(5), 831-847. <https://doi.org/10.12989/gae.2017.12.5.831>.
- Mahajan, S.P. and Budhu, M. (2009), "Shear viscosity of clays using the fall cone test", *Géotechnique*. **59**(6), 539-543. <https://doi.org/10.1680/geot.7.00114>.
- Ni, J., Hao, G.L., Chen, J.Q., Ma, L. and Geng, X.Y. (2021), "The optimisation analysis of sand-clay mixtures stabilised with xanthan gum biopolymers", *Sustainability*, **13**(7), 3732. <https://doi.org/10.3390/su13073732>.
- Ni, J., Li, S.S., Ma, L. and Geng, X.Y. (2020), "Performance of soils enhanced with eco-friendly biopolymers in unconfined compression strength tests and fatigue loading tests", *Constr. Build. Mater.* **263**, 120039. <https://doi.org/10.1016/j.conbuildmat.2020.120039>.
- Nugent, R.A., Zhang, G. and Gambrell, R.P. (2009), "Effect of exopolymers on the liquid limit of clays and its engineering implications", *Transportation Res. Record* **2101**(1), 34-43. <https://doi.org/10.3141/2101-05>.
- Reddy, N.G., Rao, B.H. and Reddy, K.R. (2018), "Biopolymer amendment for mitigating dispersive characteristics of red mud waste", *Géotech. Lett.* **8**(3), 201-207. <https://doi.org/10.1680/jgele.18.00033>.
- Rhein-Knudsen, N., Ale, M.T. and Meyer, A.S. (2015), "Seaweed hydrocolloid production: An update on enzyme assisted extraction and modification technologies", *Mar. Drugs*, **13**(6), 3340-3359. <https://doi.org/10.3390/md13063340>.
- Santos, V.P., Marques, N.S., Maia, P.C., Lima, M.A.B.D., Franco, L.D.O. and Campos-Takaki, G.M.D. (2020), "Seafood waste as attractive source of chitin and chitosan production and their applications", *Int. J. Mol. Sci.*, **21**(12), 4290. <https://doi.org/10.3390/ijms21124290>.
- Sastry, N.V., Séquaris, J.M. and Schwuger, M.J. (1995), "Adsorption of polyacrylic acid and sodium dodecylbenzenesulfonate on kaolinite", *J. Colloid Interf. Sci.*, **171**(1), 224-233. <https://doi.org/10.1006/jcis.1995.1171>.
- Smitha, S. and Sachan, A. (2016), "Use of agar biopolymer to improve the shear strength behavior of sabarmati sand", *Int. J. Geotech. Eng.*, **10**(4), 387-400. <https://doi.org/10.1080/19386362.2016.1152674>.
- Sridharan, A. and Prakash, K. (1999), "Mechanisms controlling the undrained shear strength behaviour of clays", *Can. Geotech. J.*, **36**(6), 1030-1038. <https://doi.org/10.1139/t99-071>
- Sridharan, A., Rao, S.M. and Murthy, N.S. (1988), "Liquid limit of kaolinitic soils", *Géotechnique*, **38**(2), 191-198. <https://doi.org/10.1680/geot.1988.38.2.191>.
- Tran, A.T.P., Chang, I. and Cho, G.C. (2019), "Soil water retention and vegetation survivability improvement using microbial biopolymers in drylands", *Geomech. Eng.*, **17**(5), 475-483. <https://doi.org/10.12989/gae.2019.17.5.475>.
- van de Velde, F. (2008), "Structure and function of hybrid carrageenans", *Food Hydrocolloids*, **22**(5), 727-734. <https://doi.org/10.1016/j.foodhyd.2007.05.013>.
- Venugopal, K.N. and Abhilash, M. (2010), "Study of hydration kinetics and rheological behaviour of guar gum", *Int. J. Pharma Sci. Res.*, **1**(1), 28-39. <https://doi.org/10.7439/IJASR.VIII.1.660>.
- Viswanath, S.M., Booth, S.J., Hughes, P.N., Augarde, C.E., Perlot, C., Bruno, A.W. and Gallipoli, D. (2017), "Mechanical properties of biopolymer-stabilised soil-based construction materials", *Géotech. Lett.*, **7**(4), 309-314. <https://doi.org/10.1680/jgele.17.00081>.
- Whiffin, V.S., van Paassen, L.A. and Harkes, M.P. (2007), "Microbial carbonate precipitation as a soil improvement technique", *Geomicrobiol. J.*, **24**, 417-423. <https://doi.org/10.1080/01490450701436505>.
- Wood, D.M. (1985), "Some fall cone tests", *Géotechnique*, **35**(1), 64-68. <https://doi.org/10.1680/geot.1985.35.1.64>
- Yang, J.S., Xie, Y.J. and He, W. (2011), "Research progress on chemical modification of alginate: A review", *Carbohydrate Polym.*, **84**(1), 33-39. <https://doi.org/10.1016/j.carbpol.2010.11.048>.
- Youssef, A.M., Assem, F.M., El-Sayed, S.M., Salama, H. and Abd El-Salam, M.H. (2017), "Utilization of edible films and coatings as packaging materials for preservation of cheeses", *J. Packaging Technol. Res.*, **1**(2), 87-99. <https://doi.org/10.1007/s41783-017-0012-3>.

CC